

# A collision-induced satellite in the Lyman $\beta$ profile due to H-H collisions

## Lyman $\beta$ satellites

N.F. Allard<sup>1</sup>, J. Kielkopf<sup>2</sup>, I. Drira<sup>3</sup>, and P. Schmelcher<sup>4</sup>

<sup>1</sup> Observatoire de Paris-Meudon, Département Atomes et Molécules en Astrophysique, 92195 Meudon Principal Cedex, France  
 CNRS Institut d'Astrophysique, 98 bis Boulevard Arago, 75014 Paris, France

email: allard@iap.fr

<sup>2</sup> Department of Physics, University of Louisville, Louisville, Ky 40292 U.S.A.

email: john@aurora.physics.louisville.edu

<sup>3</sup> Observatoire de Paris-Meudon, Département Atomes et Molécules en Astrophysique, 92195 Meudon Principal Cedex, France

email: Ikhlas.Drira@obspm.fr

<sup>4</sup> Institut für Physikalische Chemie, Universität Heidelberg, Im Neuenheimer Feld 229, 69120 Heidelberg, Germany

email: peter@tc.pci.uni-heidelberg.de

Received: date / Revised version: date

**Abstract.** We present a theoretical profile of the Lyman  $\beta$  line of atomic hydrogen perturbed by collisions with neutral hydrogen atoms and protons. We use a general unified theory in which the electric dipole moment varies during a collision. A collision-induced satellite appears on Lyman  $\beta$ , correlated to the  $B''\bar{B} \ ^1\Sigma_u^+ - X \ ^1\Sigma_g^+$  asymptotically forbidden transition of  $H_2$ . As a consequence, the appearance of the line wing between Lyman  $\alpha$  and Lyman  $\beta$  is shown to be sensitive to the relative abundance of hydrogen ions and neutral atoms, and thereby to provide a temperature diagnostic for stellar atmospheres and laboratory plasmas.

**PACS.** 32.70.Jz Line shapes, widths, and shifts – 52.25.Qt Emission, absorption, and scattering of ultraviolet radiation – 95.30.Dr Atomic processes and interactions – 95.30.Ky Atomic and molecular data, spectra, and spectral parameters – 97.20.Rp Faint blue stars (including blue stragglers), white dwarfs, degenerate stars, nuclei of planetary nebulae

## 1 Introduction

In Allard *et al.* 1999 [1] we derived a classical path expression for a pressure-broadened atomic spectral line shape that allows for a radiative electric dipole transition moment which depends on the position of the perturbers. This factor is not included in the more usual approximation of Anderson & Talman 1956 [2] and Baranger 1958 [3,4]. We used this theory to study the influence of the variation of the dipole moment on the satellites present in the far wing profiles of the Lyman series lines of atomic hydrogen seen in stars and in laboratory plasmas.

Satellite features at 1600 Å and 1405 Å in the Lyman  $\alpha$  wing associated with free-free quasi-molecular transitions of  $H_2$  and  $H_2^+$  have been observed in ultraviolet (UV) spectra of certain stars obtained with the International Ultraviolet Explorer (IUE) and the Hubble Space Telescope (HST) [5,6,7,8]. The stars which show Lyman  $\alpha$  satellites are DA white dwarfs, old *Horizontal Branch* stars of spectral type A, and the  $\lambda$  Bootis stars. The last two have

the distinctive property of poor *metal* content, that is, low abundances of elements other than H and He. Satellites also have been observed in the laboratory spectra of laser-produced hydrogen plasmas [9,10].

Satellite features in hydrogen lines are not limited to Lyman  $\alpha$ , which is the only Lyman-series line accessible to IUE as well as HST. Observations with HUT (Hopkins Ultraviolet Telescope) and with ORFEUS (Orbiting Retrievable Far and Extreme Ultraviolet Spectrograph) of Lyman  $\beta$  of DA white dwarfs with  $T_{\text{eff}}$  close to 20000 K have revealed a line shape very different from the expected simple Stark broadening, with line satellites near 1078 and 1060 Å [11,12]. The satellites in the red wing of Lyman  $\beta$  are in the 905 to 1187 Å spectral region covered by the Far Ultraviolet Spectroscopic Explorer (FUSE) launched in June 1999. Furthermore, Lyman  $\beta$  profiles are also the subject of an ongoing study of the far ultraviolet spectrum of dense hydrogen plasmas. The strengths of these satellite features and indeed the entire shape of wings in the Lyman series are very sensitive to the degree of ionization in the stellar atmosphere and laboratory plasmas, because

that determines the relative importance of broadening by ion and neutral collisions.

In a previous work [13] we presented theoretical profiles of Lyman  $\beta$  perturbed solely by protons. The calculations were based on the accurate theoretical  $\text{H}_2^+$  molecular potentials of Madsen and Peek [14] to describe the interaction between radiator and perturber, and dipole transition moments of Ramaker and Peek [15]. The line profiles were included as a source of opacity in model atmospheres for hot white dwarfs, and the predicted spectra compared very well with the observed ORFEUS spectra [12].

The very recent *ab initio* calculations of Drira 1999 [16] of electronic transition moments for excited states of the  $\text{H}_2$  molecule and very accurate molecular potentials of Schmelcher [17,18] now allow us to compute Lyman  $\beta$  profiles simultaneously perturbed by neutral atomic hydrogen and by protons. The aim of our paper is to point out a collision-induced satellite correlated to the  $B''\bar{B}^1\Sigma_u^+ - X^1\Sigma_g^+$  asymptotically forbidden transition of  $\text{H}_2$ . We show that the shape of the wing in the region between Lyman  $\beta$  and Lyman  $\alpha$  is particularly sensitive to the relative abundance of the neutral and ion perturbers responsible for the broadening of the lines.

## 2 Theory

The classical path theory for the shape of pressure-broadened atomic spectral lines which takes into account the variation of the electric dipole moment during a collision is only briefly outlined here. The theory has been described in detail in [1]. Our approach is based on the quantum theory of spectral line shapes of Baranger [3,4] developed in an *adiabatic representation* to include the degeneracy of atomic levels [19,20,21].

### 2.1 General expression for the spectrum in an adiabatic representation

The spectrum  $I(\omega)$  can be written as the Fourier transform of the dipole autocorrelation function  $\Phi(s)$ ,

$$I(\omega) = \frac{1}{\pi} \text{Re} \int_0^{+\infty} \Phi(s) e^{-i\omega s} ds. \quad (1)$$

Here,

$$\Phi(s) = \text{Tr} \rho \mathbf{D}^\dagger e^{\frac{is\mathbf{H}}{\hbar}} \mathbf{D} e^{-\frac{is\mathbf{H}}{\hbar}} \quad (2)$$

$$= \langle \mathbf{D}^\dagger(0) \mathbf{D}(s) \rangle \quad (3)$$

is the autocorrelation function of  $\mathbf{D}(s)$ , the dipole moment of the radiator in the Heisenberg representation (we use bold notation for operators) [22].  $\mathbf{H}$  is the total Hamiltonian

$$\mathbf{H} = \mathbf{T}_{nucl} + \mathbf{T}_{elec} + V(\mathbf{x}, \mathbf{R}), \quad (4)$$

where  $\mathbf{T}_{nucl}$  and  $\mathbf{T}_{elec}$  are sums of nuclear and electronic kinetic energy operators respectively, and  $V(\mathbf{x}, \mathbf{R})$  is the interaction between particles. Here  $\mathbf{x}$  denotes collectively

the set of electronic coordinates (position and spin) plus spin coordinates of the nuclei, while  $\mathbf{R}$  denotes the set of position coordinates of the nuclei. We assume that the radiating atom is immersed in a perturber bath in thermal equilibrium. The density matrix  $\rho$  is

$$\rho \equiv \frac{e^{-\beta\mathbf{H}}}{\text{Tr} e^{-\beta\mathbf{H}}}, \quad (5)$$

where  $\beta$  is the inverse temperature ( $1/kT$ ).

We use the notation

$$\langle (\ ) \rangle \equiv \text{Tr} \rho (\ ), \quad (6)$$

where  $\text{Tr}$  denotes the trace operation.

The adiabatic or Born-Oppenheimer representation comprises expanding states of the gas in terms of electronic states  $\chi_e(x; R)$  corresponding to frozen nuclear configurations. In the Schrödinger equation

$$\begin{aligned} (\mathbf{T}_{elec} + V(\mathbf{x}, \mathbf{R}))\chi_e(x; R) &= \mathbf{H}_{elec}(R)\chi_e(x; R) \\ &= E_e(R)\chi_e(x; R). \end{aligned} \quad (7)$$

$R$  appears as a parameter, and the eigenenergies  $E_e(R)$  play the role of potential energies for the nuclei. Any total wave function  $\Psi(x, R)$  can be expanded as

$$\Psi(x, R) = \sum_e \psi_e(R) \chi_e(x; R). \quad (9)$$

As the nuclei get far from each other, which we denote by  $R \rightarrow \infty$ , the electronic energies  $E_e(R)$  tend to asymptotic values  $E_e^\infty$  which are sums of individual atomic energies. Since atomic states are usually degenerate, there are in general several different energy surfaces which tend to a same asymptotic energy as  $R \rightarrow \infty$ . We will consider specifically a single radiating atom, the *radiator*, immersed in a gas of optically inactive atoms, the *perturbers*. For a transition  $\alpha = (i, f)$  from initial state  $i$  to final state  $f$ , we have  $R$ -dependent frequencies

$$\omega_{e'e}(R) \equiv (E_{e'}(R) - E_e(R))/\hbar, \quad e \in \varepsilon_i, e' \in \varepsilon_f \quad (10)$$

which tend to the isolated radiator frequency

$$\omega_\alpha \equiv \omega_{fi} \equiv (E_f^\infty - E_i^\infty)/\hbar \quad (11)$$

as the perturbers get sufficiently far from the radiator:

$$\omega_{e'e}(R) \rightarrow \omega_{fi} \text{ as } R \rightarrow \infty, \quad e \in \varepsilon_i, e' \in \varepsilon_f. \quad (12)$$

Let us introduce projectors  $\mathbf{P}_e$  which select the  $e^{th}$  adiabatic component of any  $\Psi(x, R)$  according to [20]

$$\mathbf{P}_e \Psi(x, R) = \psi_e(R) \chi_e(x; R). \quad (13)$$

We write the dipole moment as a sum over transitions

$$\mathbf{D} = \sum_\alpha \mathbf{D}_\alpha, \quad (14)$$

$$\mathbf{D}_\alpha \equiv \sum_{e,e'}^{(\alpha)} \mathbf{P}_{e'} \mathbf{D} \mathbf{P}_e. \quad (15)$$

In the Heisenberg representation

$$\mathbf{D}_\alpha(t) \equiv \sum_{e,e'}^{(\alpha)} e^{\frac{it\mathbf{H}}{\hbar}} \mathbf{P}_{e'} \mathbf{D} \mathbf{P}_e e^{-\frac{it\mathbf{H}}{\hbar}}, \quad (16)$$

$$\equiv \sum_{e,e'}^{(\alpha)} \mathbf{D}_{e'e}(t). \quad (17)$$

The sum  $\sum_{e,e'}^{(\alpha)}$  is over all pairs  $(e, e')$  such that  $\omega_{e',e}(R) \rightarrow \omega_\alpha$  as  $R \rightarrow \infty$ . Thus  $\mathbf{D}_\alpha$  connects all pairs of adiabatic states whose electronic energy differences become equal to  $\omega_\alpha$  as  $R \rightarrow \infty$ . In the absence of perturbers,  $\mathbf{D}_\alpha$  would be the component of  $\mathbf{D}$  responsible for the radiative transitions of frequency  $\omega_\alpha$ . We note that the projection operators account for the weighting factors discussed in Ref. [21].

Introducing the expansion Eq. (14) for  $\mathbf{D}$  into the expression Eq. (3) for  $\Phi(s)$ , we obtain

$$\Phi(s) = \sum_{\alpha,\beta} \Phi_{\alpha,\beta}(s) \quad (18)$$

where

$$\Phi_{\alpha,\beta}(s) = \text{Tr} \rho \mathbf{D}_\alpha^\dagger e^{\frac{is\mathbf{H}}{\hbar}} \mathbf{D}_\beta e^{-\frac{is\mathbf{H}}{\hbar}} \quad (19)$$

$$= \langle \mathbf{D}_\alpha^\dagger(0) \mathbf{D}_\beta(s) \rangle. \quad (20)$$

The line shape is then

$$I(\omega) = \sum_{\alpha,\beta} I_{\alpha,\beta}(\omega). \quad (21)$$

The terms  $I_{\alpha,\beta}(\omega)$ ,  $\alpha \neq \beta$ , represent interference between different spectral lines [4]. When these interference terms are neglected, we get

$$I(\omega) = \sum_{\alpha} I_{\alpha}(\omega) \quad (22)$$

and

$$\Phi(s) = \sum_{\alpha} \Phi_{\alpha}(s) \quad (23)$$

where

$$\Phi_{\alpha}(s) = \langle \mathbf{D}_\alpha^\dagger(0) \mathbf{D}_\alpha(s) \rangle. \quad (24)$$

The time dependence of  $\Phi_{\alpha}(s)$  is determined by  $\mathbf{D}_\alpha(s)$ , the part of the dipole moment which, in the absence of perturbers, oscillates at the frequency  $\omega_\alpha$ . Let us now denote

$$\mathbf{d}_\alpha(s) \equiv \mathbf{D}_\alpha(s) e^{-i\omega_\alpha s} \quad (25)$$

wherein the free evolution  $e^{-i\omega_\alpha s}$  is factored out.

For an isolated line, such as Lyman  $\alpha$ , we have shown (Allard *et al.* [1]) that the normalized line shape  $J_\alpha(\Delta\omega)$ , in the uncorrelated perturbers approximation, is given by

$$J_\alpha(\Delta\omega) = \mathbf{F} \mathbf{T} [e^{ng_\alpha(s)}] \quad (26)$$

In the classical path approximation, where we assume that the perturber follows a rectilinear trajectory at a single

mean velocity  $\bar{v}$ , we get from [21,1] that  $g_\alpha(s)$  can be written as

$$g_\alpha(s) = \frac{1}{\sum_{e,e'}^{(\alpha)} |d_{ee'}|^2} \sum_{e,e'}^{(\alpha)} \int_0^{+\infty} 2\pi\rho d\rho \int_{-\infty}^{+\infty} dx \tilde{d}_{ee'}[r(0)] [e^{\frac{i}{\hbar} \int_0^s dt V_{e'e}[r(t)]} \tilde{d}_{ee'}^*[r(s)] - \tilde{d}_{ee'}[r(0)]] \quad (27)$$

The separation of the radiator and perturber is

$r(t) = [\rho^2 + (x + \bar{v}t)^2]^{1/2}$  with  $\rho$  the impact parameter of the perturber trajectory and  $x$  is the position of the perturber along its trajectory at time  $t = 0$ . The total line strength of the transition is  $\sum_{e,e'}^{(\alpha)} |d_{ee'}|^2$ . The potential energy for a state  $e$  is

$$V_e[r(t)] = E_e[r(t)] - E_e^\infty; \quad (28)$$

the difference potential is

$$V_{e'e}[r(t)] = V_{e'}[r(t)] - V_e[r(t)]; \quad (29)$$

and we defined a *modulated* dipole [1]

$$\tilde{d}_{ee'}[r(t)] = d_{ee'}[r(t)] e^{-\frac{\beta}{2} V_e[r(t)]}, \quad (30)$$

where we denoted

$$d_{ee'}(\mathbf{r}) = \langle \chi_e(\mathbf{r}) | \mathbf{d} | \chi_{e'}(\mathbf{r}) \rangle. \quad (31)$$

In the above, we neglected the influence of the potentials  $V_e(r)$  and  $V_{e'}(r)$  on the perturber trajectories, which remain straight lines. Although we should drop the Boltzmann factor  $e^{-\beta V_e(r)}$  for consistency with our straight trajectory approximation, by keeping it we improve the result in the wings. Note that over regions where  $V_e(r) < 0$ , the factor  $e^{-\beta V_e(r)}$  accounts for bound states of the radiator-perturber pair, but in a classical approximation wherein the discrete bound states are replaced by a continuum; thus any band structure is smeared out.

## 3 Theoretical analysis

### 3.1 Formation of line satellites

Close collisions between a radiating atom and a perturber are responsible for transient quasi-molecules which may lead to the appearance of satellite features in the wing of an atomic line profile.

When the difference  $\Delta V(R)$  between the upper and lower interatomic potentials for a given transition goes through an extremum, a relatively wider range of interatomic distances contribute to the same spectral frequency, resulting in an enhancement, or *satellite*, in the line wing. The unified theory [2,22] predicts that there will be satellites centered periodically at frequencies corresponding to the extrema of the difference potential between the upper and lower states,  $\Delta\omega = k\Delta V_{\text{ext}}$ , ( $k = 1, 2, \dots$ ) [23,24,25]. Here  $\Delta\omega$  is the frequency difference between the center of the unperturbed spectral line and the satellite feature, measured for convenience in the same units as the potential energy difference. This series of satellites is due to many-body interactions.

### 3.2 Diatomic potentials

The adiabatic interaction of the neutral hydrogen atom with a proton or another hydrogen atom is described by potential energies  $V_e(R)$  for each electronic state of the  $\text{H}_2^+$  or  $\text{H}_2$  molecule ( $R$  denotes the internuclear distance between the radiator and the perturber). For H-H<sup>+</sup> collisions we have used the potentials of  $\text{H}_2^+$  calculated by Madsen and Peek [14]. For H-H collisions we have used the potentials of  $\text{H}_2$  calculated by Schmelcher [17].

In Fig. 1 we have plotted the  $\text{H}_2$  potential differences  $\Delta V(R)$  for the singlet states which contribute to Lyman  $\beta$ . We have used letters here to label the states. B3 is the well known  $B''\bar{B} \ ^1\Sigma_u^+$  state. At small internuclear separation,  $R$ , the state correlates with the  $B'' \ ^1\Sigma_u^+$  state, the third  $^1\Sigma_u^+$  state of the Rydberg series. At larger internuclear separation the state has an ionic character until  $R=19 \text{ \AA}$  where the potential energy curve of the  $\text{H}^+ + \text{H}^- (1s)^2$  state crosses the  $\text{H}(n=1) + \text{H}(n=3)$  energy levels, because of an avoid crossing  $\bar{B}$  loses its ionic character. Dabrowski and Herzberg [26] predicted the existence of the  $\bar{B}$ , the first calculations were done by Kolos [27,28]. More recent calculations are reported in [18,29].

We use B4 and B5 respectively to label the  $4 \ ^1\Sigma_u^+$  and  $5 \ ^1\Sigma_u^+$  states, and V and D to label the  $3 \ ^1\Pi_u$  and  $2 \ ^1\Pi_u$  states.

Each difference potential exhibits at least one extremum which, in principle, leads to a corresponding satellite feature in the wing of Lyman  $\beta$  (see Sect. 3.1). The present approach now allows us also to take into account the asymptotically forbidden transitions of quasi-molecular hydrogen which dissociate into (1s,3s) and (1s,3d) atoms. The satellite amplitude depends on the value of the dipole moment through the region of the potential extremum responsible of the satellite and on the position of this extremum. We have shown [1,13,30] that a large enhancement in the amplitude of a spectral line satellite occurs whenever the dipole moment increases through the region of internuclear distance where the satellite is formed.

The potential differences of the B3-X and B4-X transitions exhibit double wells. The maximum at  $3.0 \text{ \AA}$  of the B3-X potential and minimum of the B4-X potential are due to an avoided-crossing.

The most significant characteristic of Fig. 1 is the existence of the deep outer well at  $6 \text{ \AA}$  of the B3-X potential. The ionic interaction decays slowly making the potential energy difference very broad compared to the very steep wells of the other transitions. This is very important as the position of the extremum and the functional dependence of the potential difference on internuclear separation determine the amplitude and shape of the satellites [21].

### 3.3 Electronic transition dipole moments

The dipole moment taken between the initial and final states of a radiative transition determines the transition probability, but for two atoms in collision, the moment depends on their separation. This modifies relative contributions to the profile along the collision trajectory. Dipole

moments for  $\text{H}_2^+$  and  $\text{H}_2$ , calculated as a function of internuclear distance respectively by Ramaker and Peek [15] and by Drira [16], were used for the transitions contributing to Lyman  $\alpha$  and Lyman  $\beta$ . For Lyman  $\beta$ , the four components which correspond to  $1s-3p$  atomic transitions are dipole allowed [16]: the two singlet B4-X and D-X transitions, and the two triplet  $4 \ ^3\Sigma_g^+ - 3 \ ^3\Sigma_u^+$  and  $2 \ ^3\Pi_g - 3 \ ^3\Sigma_u^+$  transitions.

If electronic states  $i$  and  $f$  of an isolated radiator are not connected by the dipole moment operator, that is if  $D_{if}(R \rightarrow \infty) = 0$ , allowed radiative transitions cannot occur between these two states. This happens for the other transitions which correspond to  $1s-3s$  and  $1s-3d$  atomic transitions. Although these transitions should not contribute to the unperturbed line profile,  $D_{if}(R)$  may differ from zero when a perturber passes close to the radiator. In this instance radiative transitions are induced by collisions, but not at the unperturbed line frequency.

It often arises that an extremum in the potential difference occurs when the final (or initial) potential energy curve exhibits an avoided crossing, the corresponding wavefunctions exchange their characteristics and the radiative dipole transition moment varies dramatically with  $R$ . This is exactly what happens for the B3-X transition. To point out the importance of variation of dipole moment on the formation of a collision-induced (CI) satellite, we have displayed in Fig. 2  $D(R)$  together with the corresponding  $\Delta V(R)$  for the B3-X asymptotically forbidden transition. The dipole transition is extremely small for the isolated radiating atom ( $R \rightarrow \infty$ ) but it goes through a maximum at the value of  $R$  where the avoid-crossing occurs and remains quite important at the internuclear distance where the potential difference of the outer well goes through a minimum.

In such a case we expect a contribution from this transition in the wing and the formation of a CI line satellite, if it is not smeared out by larger dipole-allowed contributions.

## 4 Lyman $\beta$ profile

The Lyman profiles and satellites shown here are calculated at the low densities met in the atmospheres of stars. The typical particle densities from  $10^{15}$  to  $10^{17} \text{ cm}^{-3}$  allows us to use an expansion of the autocorrelation function in powers of density as described in [21,31]. Line profiles are normalized so that over  $\omega$  they integrate to 1.

### 4.1 Collisional profile perturbed by neutral H

We will consider the two following mechanisms which contribute to the Lyman  $\beta$  wing.

- The far wing of allowed dipole lines, due to the free-free transition in a pair of colliding atoms.
- The collision-induced absorption due to the free-free transition involving the transient dipole moment existing during a binary collision.

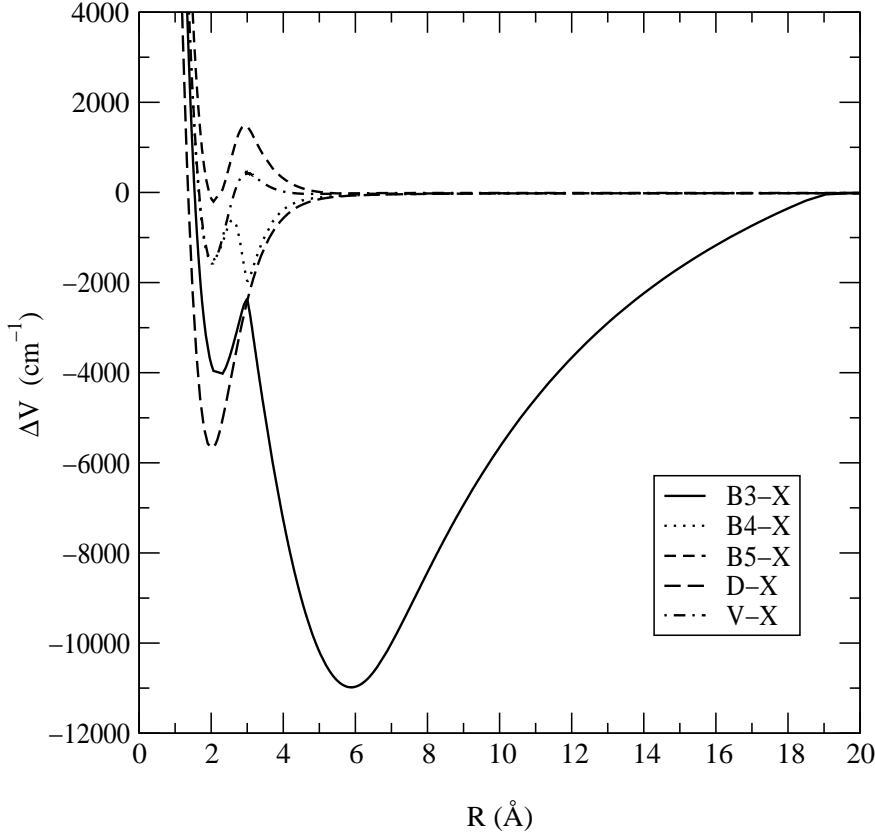


**Fig. 1.** Difference potential energies expressed in  $\text{cm}^{-1}$  for the singlet states of  $\text{H}_2$  contributing to Lyman *beta*.

The line profile calculation shown Fig. 3 has been done at a temperature of 10000 K for a perturber density of  $10^{16} \text{ cm}^{-3}$  of neutral hydrogen. The only line feature is a broad CI satellite situated at  $1150 \text{ \AA}$  in the far wing, due to the B3-X dipole forbidden transition. Normally such an effect would be overshadowed by the allowed transition wing, but in this case there is no large contribution of the dipole allowed transitions in this region, as can be easily predicted by the examination of Fig. 1. The extrema of the allowed B4-X and D-X transitions occur for very short distances, and are much smaller compared to the position and depth of the outer well in the B3-X transition (see Sect. 3.1 and 3.2).

The collision-induced absorption depends on the internuclear separation and produces very broad spectral lines with a characteristic width of the order of the inverse of the duration of the close collision. It is strongly dependent on

- the temperature
- the amplitude of the dipole for  $R_{\min}$  when the potential difference presents a minimum.

This emphasizes the importance of the accuracy of both the potential energies *and* the dipole moments for the line shape calculations.

Oscillatory structures appear near the  $1150 \text{ \AA}$  satellite as they appear between the line and the  $1600 \text{ \AA}$  satellite in both theory and experiment [1]. These oscillations were predicted by Royer [32] and Sando *et al.* [33,34].

#### 4.2 Simultaneous perturbations by H and $\text{H}^+$

The complete Lyman  $\beta$  profile perturbed by collisions with neutral hydrogen and protons is shown in Fig 3. We notice that the collision-induced H-H satellite is much broader than the allowed H- $\text{H}^+$  satellite since the dipole moment differs from zero only over a short range of internuclear distances (see Sect. 4.1). The CI satellite of Lyman  $\beta$  is quite far from the unperturbed Lyman  $\beta$  line center, actually closer to the Lyman  $\alpha$  line. It is therefore necessary to take into proper account the total contribution of both the Lyman  $\alpha$  and Lyman  $\beta$  wings of H perturbed simultaneously by neutrals and protons and to study the variation

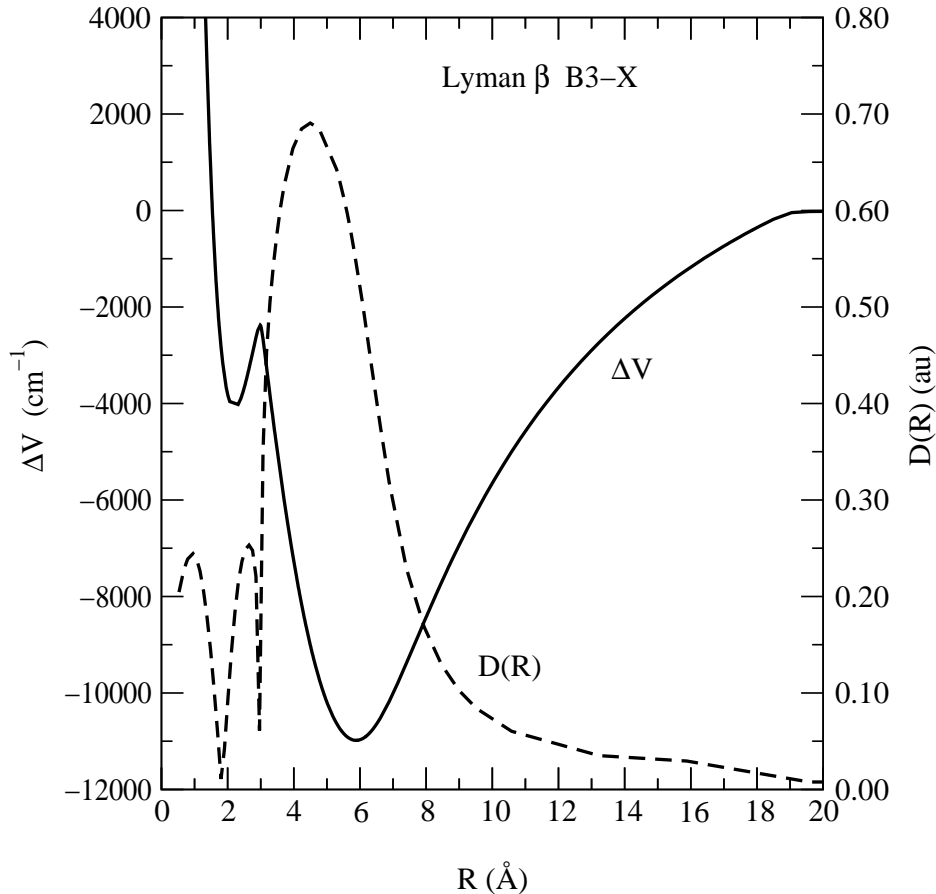


**Fig. 2.** Difference potential energy  $\Delta V$  in  $\text{cm}^{-1}$  and the corresponding  $D(R)$  in atomic units for the dipole forbidden B3-X transition which gives the CI satellite of Lyman  $\beta$ .

of this part of the Lyman series with the relative density of ionized and neutral atoms.

In [1] we evaluated both the Lyman  $\alpha$  and Lyman  $\beta$  wings of H perturbed by protons. However, we neglected interference terms between the two lines. Equation (51) of [1], which gives the profile for a pair of lines such as Lyman  $\alpha$  and  $\beta$ , is

$$I(\omega) = \phi_{\alpha}^{(0)} e^{nf_{\alpha}(0)} J_{\alpha}(\omega - \omega_{\alpha}) + \phi_{\beta}^{(0)} e^{nf_{\beta}(0)} J_{\beta}(\omega - \omega_{\beta}). \quad (32)$$

The perturbed line strength  $\phi_{\alpha}^{(0)} e^{nf_{\alpha}(0)}$  differs from the free line strength  $\phi_{\alpha}^{(0)}$  by the factor  $e^{nf_{\alpha}(0)}$ . This density-dependent factor expresses the fact that the total intensity radiated increases or decreases when the dipole moment is increased or decreased, on average, by the proximity of perturbers. Because of the low densities we consider, we have neglected this factor here.

We show the sum of the profiles of Lyman  $\alpha$  and Lyman  $\beta$  in Fig. 4. We can see that a ratio of 5 between the neutral and proton density is enough to make the CI

satellite appear in the far wing. The CI satellite appearance is then very sensitive to the degree of ionization and may be used as a temperature diagnostic.

## 5 Conclusions

In the case of Lyman  $\alpha$  and the H-H<sup>+</sup> Lyman  $\beta$  satellites, the potential shape played a dominant role in the large difference in the broadening of the quasi-molecular features [30]. The width of the collision-induced absorption is determined, for the most part, by the short range over which the corresponding transition dipole moment is significant. In the CI satellite, it is the dipole moment which is very important and which is responsible of the shape of the satellite, the observation of such a satellite would be a test of the accuracy of the dipole moment calculation. Satellites due to allowed and forbidden transitions depend linearly on density. The CI satellite is very sensitive to the temperature of the absorption, and it may also be used as a diagnostic tool for temperature. We emphasize that the

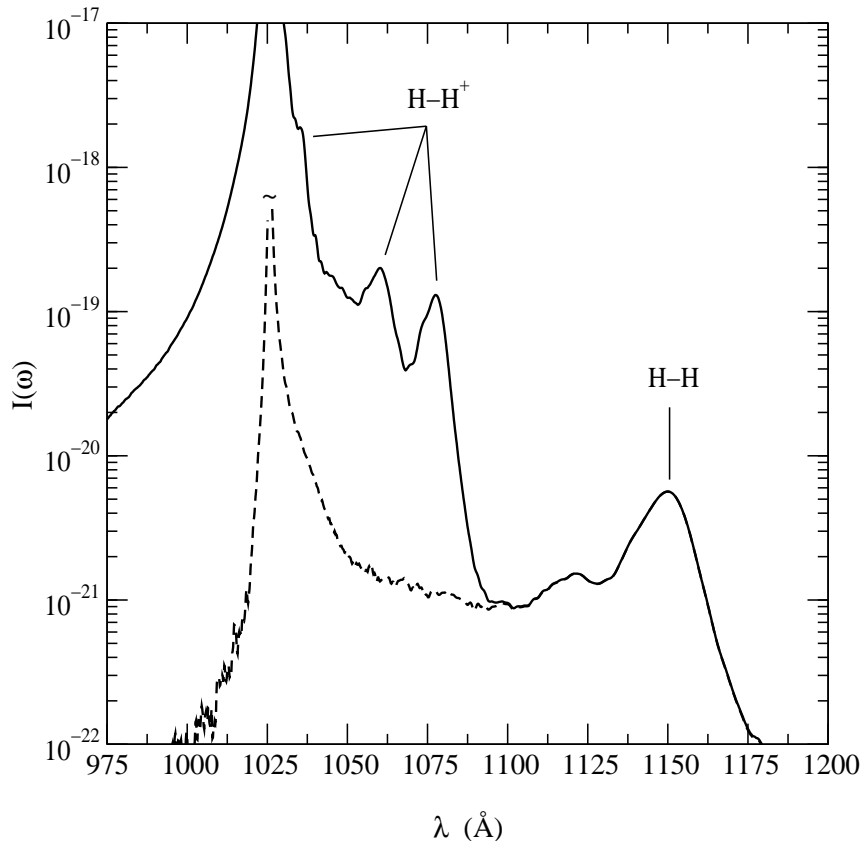


**Fig. 3.** Line profile of Lyman  $\beta$  perturbed by neutral hydrogen and protons. The dashed line (---) shows only the contribution from neutral perturbers.

effect of finite collision duration does play a role in the shape of the far wing. The present calculations are done in an adiabatic approximation using a rectilinear trajectory. This should affect slightly the shape of the satellite, although no great error is expected. We are developing methods to include trajectory effects in the evaluation of the line shape.

## Acknowledgements

The computations of dipole transition moments were performed on the CRAY of the computer center IDRIS. The work at the University of Louisville is supported by a grant from the U.S. Department of Energy, Division of Chemical Sciences, Office of Basic Energy Sciences, Office of Energy Research.

## References

1. N.F. Allard, A. Royer, J.F. Kielkopf, N. Feautrier, Phys. Rev. A **60**, 1021 (1999).
2. P.W. Anderson, J.D. Talman, Bell System Technical Publication No. 3117 (Murray Hill, NJ, 29 1956).
3. M. Baranger, Phys. Rev. **111**, 481 (1958).
4. M. Baranger, Phys. Rev. **111**, 494 (1958).
5. D. Koester, N.F. Allard, in *White Dwarfs: Advances in Observation and Theory*, edited by M. Barstow (Kluwer, Dordrecht, 1993), p. 237.
6. D. Koester, N.F. Allard, G. Vauclair, Astron. Astrophys. **291**, L9 (1994).
7. H. Holweger, D. Koester, N.F. Allard, Astron. Astrophys. **290**, L21 (1994).
8. P. Bergeron, F. Wesemael, R. Lamontagne, G. Fontaine, R. Saffer, N.F. Allard, Astrophys. J. **449**, 258 (1995).
9. J.F. Kielkopf, N.F. Allard, Astrophys. J. **450**, L75 (1995).
10. J.F. Kielkopf, N.F. Allard, Phys. Rev. A **58**, 4416 (1998).
11. D. Koester, D.S. Finley, N.F. Allard, J.W. Kruk, R.A. Kimble, Astrophys. J. **463**, L93 (1996).
12. D. Koester, U. Sperhake, N.F. Allard, D.S. Finley, S. Jordan, Astron. Astrophys. **336**, 276 (1998).
13. N.F. Allard, J.F. Kielkopf, N. Feautrier, Astron. Astrophys. **330**, 782 (1998).

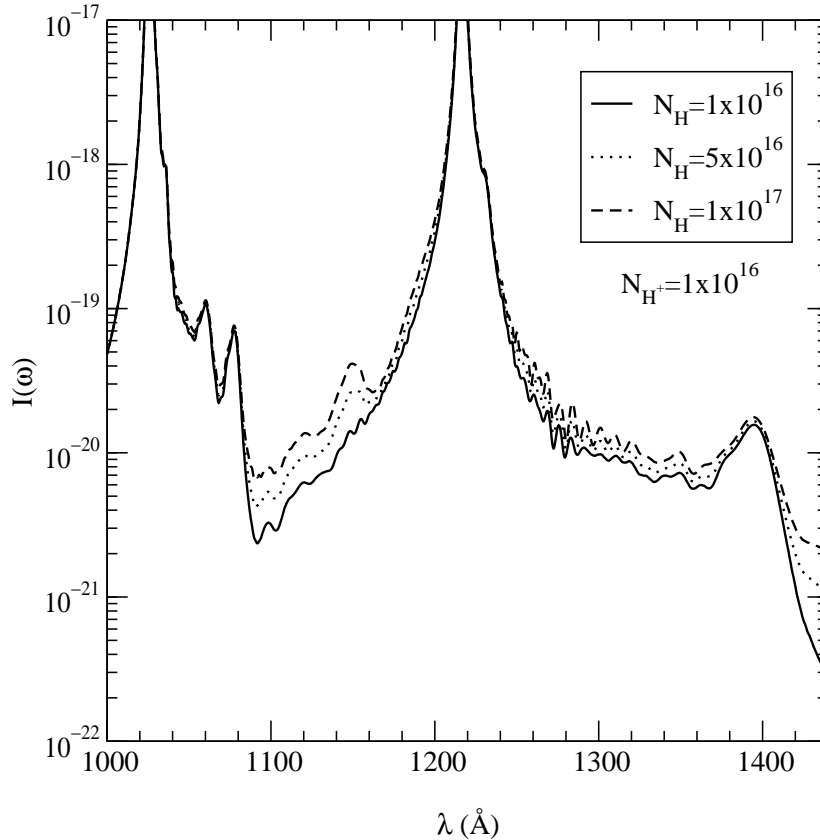


**Fig. 4.** Total profile of Lyman  $\alpha$  and Lyman  $\beta$  perturbed by neutral hydrogen and protons. Three different neutral densities ( $1 \times 10^{16}$ ,  $5 \times 10^{16}$ ,  $1 \times 10^{17}$   $\text{cm}^{-3}$ ) are compared for a fixed ion density ( $1 \times 10^{16}$   $\text{cm}^{-3}$ ).

14. Madsen M.M., Peek J.M., *Atomic Data* **2**, 1971, 171.
15. Ramaker D.E., Peek J.M., *J. Phys. B* **5**, 1972, 2175.
16. Drira, I., *J. Mol. Spectroscopy* **198**, 52 (1999).
17. Schmelcher, P., private communication.
18. T. Detmer, P. Schmelcher, L.S. Cederbaum, *J. Chem. Phys.* **109**, 9694 (1998).
19. A. Royer, *Can. J. Phys.* **52**, 1816 (1974).
20. A. Royer, *Phys. Rev. A* **22**, 1625 (1980).
21. N.F. Allard, D. Koester, Feautrier N., Spielfiedel A., *Astron. Astrophys. Suppl. Ser.* **108**, 417 (1994).
22. N.F. Allard, J. Kielkopf, *Rev. Mod. Phys.* **54**, 1103 (1982).
23. N.F. Allard, *J. Phys. B* **11**, 1383 (1978).
24. A. Royer, *Acta Phys. Pol. A* **54**, 805 (1978).
25. J.F. Kielkopf, N.F. Allard, *Phys. Rev. Lett.* **43**, 3 (1979).
26. I. Dabrowski, G. Herzberg, *Can. J. Phys.* **54**, 525 (1976).
27. W. Kolos, *J. Mol. Spectroscopy* **62**, 429 (1976).
28. W. Kolos, *J. Mol. Spectroscopy* **86**, 420 (1981).
29. Reinhold E., Hogervorst W., Ubachs W., Wolniewicz L., *Phys. Rev. A* **60**, 1258 (1999)
30. N.F. Allard, I. Drira, M. Gerbaldi, J.F. Kielkopf, A. Spielfiedel, *Astron. Astrophys.* **335**, 1124 (1998).
31. A. Royer, *Phys. Rev. A* **3**, 2044 (1971).
32. A. Royer, *Phys. Rev. A*, **43**, 499 (1971).
33. Sando K.M., Doyle R.O., Dalgarno A., *Astrophys. J.* **157**, L143 (1969).
34. Sando K.M., Wormhoudt J.G., *Phys. Rev. A* **7**, 1889 (1973).